Hindawi
Complexity
Volume 2019, Article ID 5234382, 10 pages
https://doi.org/10.1155/2019/5234382

Research Article

Chaotic Dynamics of an Airfoil with Higher-Order Plunge and Pitch Stiffnesses in Incompressible Flow

Karthikeyan Rajagopal, Yesgat Admassu, Riessom Weldegiorgis, Prakash Duraisamy, and Anitha Karthikeyan

Center for Nonlinear Dynamics, Institute of Research and Development, Defence University, Bishoftu, Ethiopia

Correspondence should be addressed to Karthikeyan Rajagopal; rkarthiekeyan@gmail.com

Received 15 June 2019; Revised 14 September 2019; Accepted 1 October 2019; Published 30 October 2019

Guest Editor: Lazaros Moysis

Dynamical properties of a two-dimensional airfoil model with higher-order strong nonlinearities are investigated. Firstly, a state-space model is derived considering the plunge and pitch stiffnesses as generalized functions. Then, a stiffness function having square, cubic, and fifth-power nonlinearities is considered for both plunging and pitching stiffnesses, and the dimensionless state equations are derived. Various dynamical properties of the proposed model are investigated using equilibrium points, eigenvalues, and Lyapunov exponents. To further analyze the dynamical behavior of the system, bifurcation plots are derived. It is interesting to note that the new airfoil model with higher-order nonlinearities shows multistability with changing airspeed, and there are infinitely countable number of coexisting attractors generally called as megastability. Both multistability and megastability features of the airfoil model were not captured earlier in the literatures. To be clear, it is the first time a megastable feature is exposed in a physical system. Finally, to analyze the multifrequency effects of the airfoil model, we have presented the bicoherence plots.

1. Introduction

Many literatures have shown that the airfoil (aeroelastic) systems show more complex dynamical behaviors such as limit cycles and chaotic oscillations [1–4]. A persistent flutter in an aeroelastic structure such as an aircraft wing may create dangerous effects to the structure and may cause structural unstability [1, 2]. Hence, controlling such unwanted and persistent oscillations has attracted importance among researchers [2–4]. A dynamical model of an airfoil system with cubic nonlinearity considered for the pitching stiffness was proposed in [5, 6], and it is shown that the system exhibits chaotic oscillations when the airspeed crosses a critical limit. A rigid wing supported by a nonlinear spring shows limit cycles as discussed in [7]. The authors investigated piecewise nonlinearities in aeroelastic systems, and the authors address continuous nonlinearities such as those found in structural systems that exhibit spring hardening or softening effects.

A nonlinear active control method is adopted to control the limit cycle oscillations of an aeroelastic system with quasi-steady aerodynamic models [8, 9]. However, the results are limited to the elevation condition, and the real case should also be considered the actual vibration state and hence, the dynamic state must be set within an internal dynamic state when the nonlinear controller is designed [10]. In [11], a two-dimensional airfoil system with pitch and plunge stiffnesses using subsonic aerodynamics theory and classical nonlinearities, namely, cubic, freeplay, and hysteresis is investigated. Several cases of aerodynamic nonlinearities arising from transonic flow and dynamic stall are discussed, and numerical simulations are conducted. Poincaré mapping method and Floquet theory are adopted to analyze the limit cycle oscillation flutter and chaotic motion of a two-dimensional airfoil system with combined freeplay and cubic pitch stiffnesses in supersonic and hypersonic flows [12]. It is shown that the Floquet theory can effectively predict the occurrence of limit cycles in the system.

In [13, 14], the aeroelastic airfoil system with freeplay is investigated and the transonic flow characteristics are discussed. The effect of hardening and nonlinearities on aeroelastic system is analyzed in [15]. The chaotic behavior and prediction of it with various methods and its robustness are presented in [16]. The comparative study reveals the effectiveness of Runge–Kutta method over other methods. A two-degree-of-freedom model of airfoil system is derived, and analysis is carried out to study the consequences of cubic nonlinearities [17]. Drastic changes are observed while the system entered to supersonic flow. Using precise integration method the nonlinear effect on airfoil system is simulated in [18]. The results show the presence of intricate behaviors of the system. The investigation on limit cycle oscillation and other aeroelastic responses is described in [19, 20] for system with freeplay in pitch. Challenges and complications during control and design of vibration absorber are discussed elaborately for the aeroelastic model with nonlinearities in [21, 22].

An airfoil model with multiple strong nonlinearities for both pitch and plunge stiffnesses was studied, and incremental harmonic balance method was used to analyze the periodic state of the airfoil flutter [26]. Similarly, to analyze such periodic oscillations in an airfoil system, Monte Carlo method was adopted in [27]. A nonlinear adaptive control technique is used to suppress the flutter and limit cycle oscillations assuming that one state is known and the other states are compensated [28]. A terminal sliding-mode control technique is used to suppress the limit cycle oscillations with an exclusive choice between the plunge displacement and the pitch angle [29]. Differential transformation method (DTM) to examine the nonlinear dynamic response of a typical aeroelastic system with cubic nonlinearities for pitch stiffness under realistic operating parameters was proposed in [30], and the dynamical properties are investigated with bifurcation plots and Lyapunov spectrum. A nonlinear sliding-mode controller was designed to suppress the chaotic oscillations of an airfoil system proposed in [10], and the stability of the controllers was derived using the Lyapunov stability theorem [31]. A nonlinear energy sink (NES) is used to suppress the aeroelasticity of an airfoil with a control surface considering the freeplay and cubic stiffnesses in pitch. The harmonic balance method is used to determine the limit cycle oscillations occurring in the airfoil-NES system [32].

In [29], the authors mentioned that a constant deterioration of wing structure influences on stiffness behavior, which demands higher-order nonlinearity in the dynamic model. In [33], influence of higher-order stiffness on aeroelastic model was discussed but no special properties are analyzed. Motivated by the above discussions, we are interested in exploring the airfoil system considering both plunge and pitch stiffnesses to be higher-order nonlinearities. This paper reports some new complex behaviors of the airfoil system like multistability and megastability which have not been reported earlier in the literatures. The proposed investigation falls under category 1 and 2 as described in [34].

2. Two-Dimensional Airfoil System with Higher-Order Nonlinear Spring (ASHS)

2.1. Mathematical Model. The dynamical model of an airfoil with cubic pitching stiffness and viscous damping as shown in Figure 1 was proposed in [5, 6]. ρ is the air density, m is the mass, b is the semichord length, ab is the distance of the elastic axis E from the midchord point, $(0.5 + a)b$ is the distance of E from the aerodynamic focus F, $x_\alpha b$ is the distance of the center of gravity from E, $r_a b$ is the radius of gyration of the airfoil with respect to E, and ω_h and ω_α are the eigenfrequencies of the constrained one-degree-of-freedom system associated with the linear plunging and the pitching springs, respectively. The parameter values are considered as follows: $a = -0.1$, $b = 1$ m, $x_a = 0.25$, $r_a^2 = 0.5$, $\omega_h = 28.1$ Hz, and $\omega_\alpha = 62.8$ Hz.

The bifurcation analysis of the proposed model [5, 6] was investigated using harmonic balance method. It is to be noted that the literatures have investigated the dynamical behavior of the airfoil system using cubic nonlinearity stiffness. Such approximations of the nonlinear stiffness have not been useful in identifying the more complex behavior of the system. Hence, we propose a modified dynamical equation of the airfoil system as

$$\begin{aligned} \ddot{h} + 0.25\ddot{\alpha} + 0.1\dot{h} + 0.2h + 0.1\beta\alpha + f(h) &= 0, \\ 0.25\ddot{h} + 0.5\ddot{\alpha} + 0.1\dot{\alpha} + 0.5\alpha - 0.04\beta\alpha + f(\alpha) &= 0, \end{aligned} \tag{1}$$

where $f(\alpha)$ is the pitching stiffness and $f(h)$ is the plunging stiffness. The state h represents the plunging displacement, and α represents the pitching angle. The parameter $\beta = (V/b\omega_\alpha)^2$, where V is the airspeed and ω_α is the eigenfrequency.

With higher-order nonlinear stiffness in an aeroelastic system, limit cycle oscillations occur, which leads to a fatigue in the wing structure as the consequence of a long-term vibration with constant amplitude at an invariant frequency [29]. In [35], the 5th order nonlinearity is introduced and its effects are analyzed; the authors observed that the resonant frequency is shifted toward higher frequency and the bandwidth of higher-order stiffness is wider for frequency up-sweeps. It is very clear that the 5th order nonlinearity increases the complexity, and its effects need to be studied.

In this paper, we consider higher-order pitching and plunging stiffnesses in order to investigate the complex behaviors which have not been reported earlier.

Using $x = \alpha, \dot{x} = y, z = h$, and $\dot{z} = w$, we derive the dimensionless model as

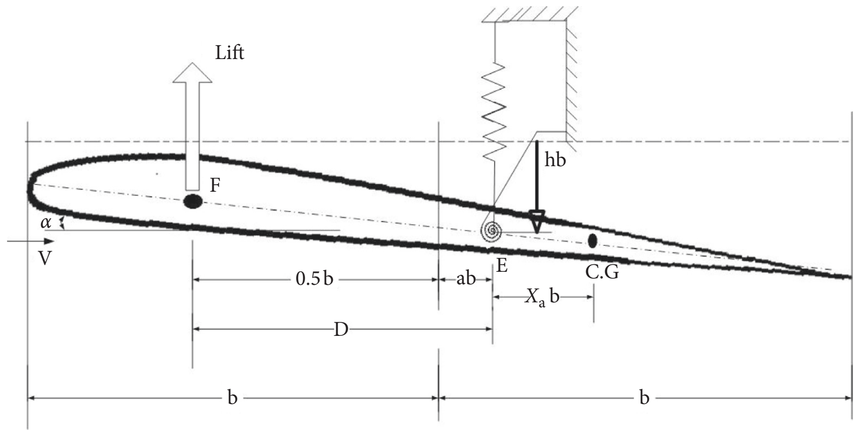

FIGURE 1: Two-degree-of-freedom airfoil model.

$$
\begin{aligned}
\frac{dx}{dt} &= y,\\
\frac{dy}{dt} &= \frac{1}{1.75}\left(4x(0.065\beta - 0.5) + 0.1w + 0.2z + f(z)\right.\\
&\quad \left. - 4f(x) - 0.4y\right),\\
\frac{dz}{dt} &= w,\\
\frac{dw}{dt} &= -\frac{1}{1.75}\left(x(0.24\beta - 0.5) + 0.2w + 0.4z + 2f(z)\right.\\
&\quad \left. - f(x) - 0.1y\right),
\end{aligned}
\tag{2}
$$

where $f(z) = 5z^2 + 10z^3 + 40z^5$ and $f(x) = 5x^2 + 20x^3 + 40x^5$ are the higher-order stiffnesses. The parameter β is considered as the bifurcation parameter, and for a fixed value of the airspeed, $\beta = 7.5$, and for the initial conditions $[0.1, 0, 0.1, 0]$, the phase portraits of the system are shown in Figure 2.

2.2. Existence of Attractor. It has been proved in the literatures that nonlinear dissipative systems can produce chaotic attractors. Hence, to show that the ASHS is dissipative, we have computed the corresponding volume contraction rate V_c, using summation of Lyapunov exponents (i.e., $V_c = L.E_1 + L.E_2 + L.E_3 + L.E_4$), and thus, if $V_c < 0$, the system is dissipative, thus experiences or presents attractors. For $V_c = 0$, phase space volume is conserved and the dynamical system is conservative. If $V_c > 0$, the volume in phase space expands, and hence there exist only unstable cycles or possibly chaotic repellors.

For ASHS, $L.E_1 = 0.2014, L.E_2 = 0, L.E_3 = 0.1852$, and $L.E_4 = 0.1852$. It can be observed that $V_c = -0.169 < 0$ for all state vectors; thus, the introduced system is dissipative.

2.3. Stability of Equilibrium Points. In order to obtain the equilibrium of our model, let $\dot{x} = \dot{y} = \dot{z} = \dot{w} = 0$; then, the only real equilibrium point of ASHS is at the origin.

The Jacobian matrix of the ASHS system evaluated at any equilibrium is given by

$$
\begin{aligned}
J(X) &= \begin{bmatrix} 0 & 1 & 0 & 0 \\ a_1 & a_2 & a_3 & a_4 \\ 0 & 0 & 0 & 1 \\ a_5 & a_6 & a_7 & a_8 \end{bmatrix},\\
a_1 &= \frac{26\beta}{175} - \frac{160x}{7} - \frac{960x^2}{7} - \frac{3200x^4}{7} - \frac{8}{7},\\
a_2 &= \frac{-8}{35},\\
a_3 &= \frac{800z^4 + 120z^2 + 40z}{7} + \frac{4}{35},\\
a_4 &= \frac{2}{35},\\
a_5 &= \frac{800x^4 + 240x^2 + 40x}{7} - \frac{24\beta}{175} + \frac{2}{7},\\
a_6 &= \frac{2}{35},\\
a_7 &= -\frac{80z - 240z + \left(1600z^4\right)}{7} - \frac{8}{35},\\
a_8 &= \frac{-4}{35}.
\end{aligned}
\tag{3}
$$

The eigenvalues associated with the above Jacobian matrix are obtained by solving the following characteristic equation $(\det(M_J - \lambda I_d) = 0)$, where I_d is the identity matrix:

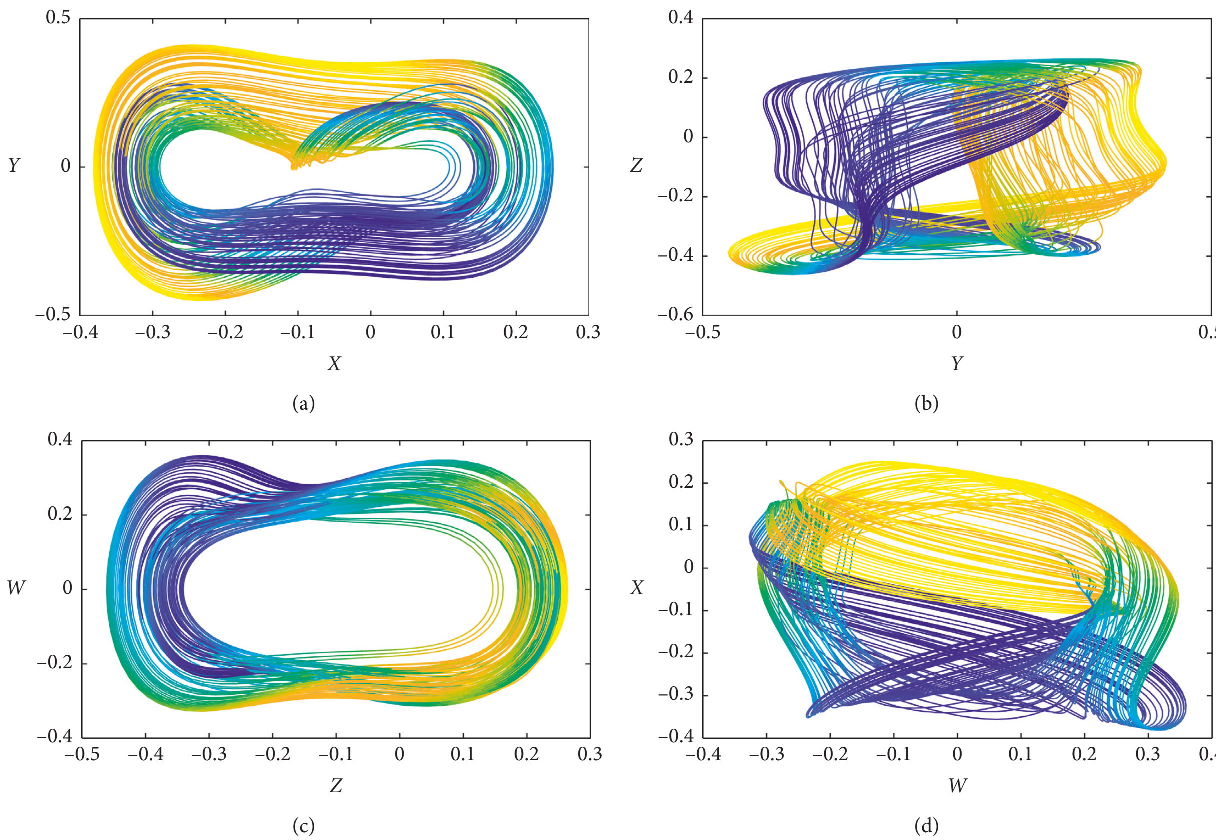

FIGURE 2: 2D phase portraits of the ASHS.

$$\lambda^4 + 0.342\lambda^3 + (1.39 - 0.148\beta)\lambda^2 + (0.16 - (9.14e - 3)\beta)\lambda - 0.0182\beta + 0.229 = 0. \tag{4}$$

Figure 3 shows the stability of the equilibrium point for various values of β. It is to be noted that the system shows unstable oscillations when the airspeed exceeds the critical divergent speed $\beta \geq 4.08015$ which agrees with the results described in [5].

From the Routh–Hurwitz stability criterion, the stability conditions of all the principal minors need to be positive for the ASHS system to be stable. The principal minors are as folows:

$$\begin{aligned}
\Delta_1 &= \delta_1 > 0,\\
\Delta_2 &= \begin{vmatrix} \delta_1 & \delta_0 \\ \delta_3 & \delta_2 \end{vmatrix} > 0,\\
\Delta_3 &=> \begin{vmatrix} \delta_1 & \delta_0 & 0 \\ \delta_3 & \delta_2 & \delta_1 \\ 0 & 0 & \delta_3 \end{vmatrix} > 0,
\end{aligned} \tag{5}$$

that is, $\delta_1 > 0$, $\delta_1\delta_2 - \delta_3 > 0$, and $\delta_3 > 0$, where $\delta_1 = 0.342$, $\delta_2 = (1.39 - 0.148\beta)$, and $\delta_3 = 0.16 - (9.14e - 3)\beta$, where the conditions are satisfied; then, ASHS is stable, leading to the situation of point attractor; otherwise, the system is unstable, and the model can experience periodic or chaotic oscillations.

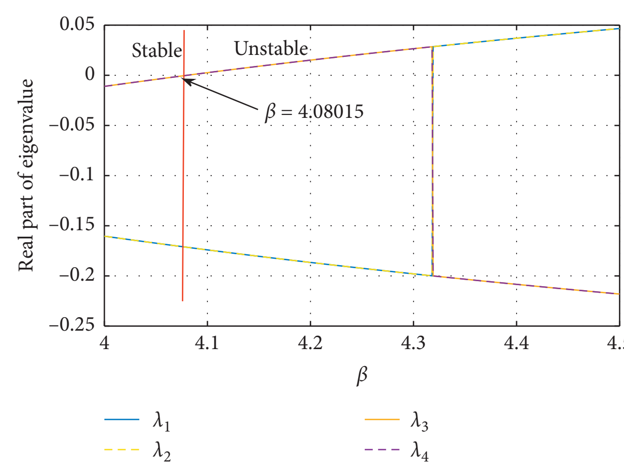

FIGURE 3: Stability of the equilibrium point for various values of β.

3. Numerical Simulation

3.1. Bifurcation and Multistability. The bifurcation plots are derived and investigated to study the impact of the parameters on the system behavior. The parameter β is considered as the bifurcation parameter with the other parameters fixed at their respective chaotic values. The initial condition for the first iteration is taken as $[0.1, 0, 0.1, 0]$. Multistability in physical systems is already discussed in the literatures [36, 37], and it is shown that such coexisting oscillations are dangerous and can affect the structural stability of a system.

To show the existence of multistability, we use a robust way to plot the bifurcation plots where the initial conditions are changed in every iteration to the end values of the state variables wherein the parameter is increased or decreased in tiny steps. It is to be noted that the airfoil system shows multistability as shown in Figure 4 which was not reported earlier in the literatures.

Figure 4 (blue) shows the forward continuation where the parameter β is increased from minimum to maximum, and Figure 4 (red) shows the backward continuation where the parameter β is decreased from maximum to minimum, and the local maxima of the state variables are plotted. The corresponding Lyapunov exponents (LEs) are calculated using Wolf's algorithm [38] for a finite time of 40,000 s. It should be noted that we used the same forward and backward continuation to generate the Lyapunov spectrum for β. Figures 5(a) and 5(b) show the LEs for forward and backward continuation.

The ASHS system takes a period-doubling route to chaos as shown in Figure 6. Also, we could see the period-doubling route to chaos for $\beta \geq 6$ and an inverse period-doubling exit from chaos for $4.7 \leq \beta \leq 5.3$. Such a phenomenon of period doubling and inverse period doubling occurring in a bifurcation diagram is termed as antimonotonicity [39].

Different two-dimensional projections of the ASHS attractor are presented in Figure 6. We can easily note that there is no linear dependency between the state variables of the ASHS and also such dependencies between state vectors can be nonlinear and can involve several of the variables.

From Figures 4 and 5, it is evident that the ASHS shows coexisting attractors. We have plotted the 2D phase portraits of the coexisting attractors for different values of initial conditions and parameter β. It can be seen that a period-1 limit cycle (red) coexists with a chaotic attractor (blue) (Figure 7).

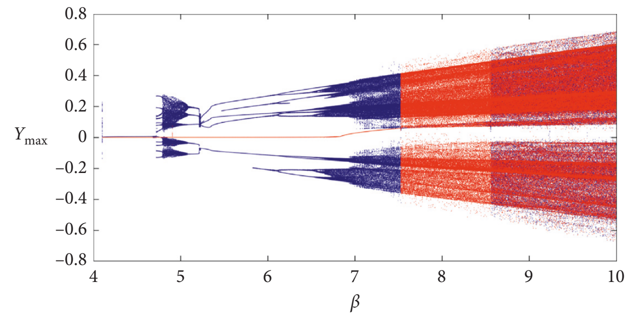

Figure 4: Maximum of ASHS with forward (red) and backward (blue) continuation.

3.2. Megastability. It was Sprott et al. who introduced the term "megastability" which is defined as the coexistence of a countable infinity of attractors in a system. He proposed a system which is a periodically-forced oscillator with a spatially-periodic damping term [40]. The system looks like a cross-sectioned cabbage with multiple layers of periodic, quasiperiodic, and chaotic attractors. A new oscillator with infinite coexisting asymmetric attractors with the megastability property was proposed in [41], in which the attractors are a combination of self-excited and hidden attractors. A two-dimensional chaotic oscillator producing a whirlpool of attractors was proposed in [42]. Similarly, Tang et al. proposed a chaotic system with coexisting attractors which forms a carpet-like structure [43]. To show the controllability of such megastable oscillators, the authors in [44] have proposed a fuzzy-based control algorithm to suppress chaotic oscillations. Most of these oscillators use a periodic forcing term and it was in [45], the forcing term was modified to a quasiperiodic function and was proved that the quasiperiodic forcing can also produce megastable oscillators. It is to be noted that, in the entire literatures on megastable oscillators, there were no discussions on such megastability in a real physical system. The proposed ASHS model discussed in this paper shows such megastability as shown in Figure 8 for $\beta = 7$ and different initial conditions.

3.3. Bicoherence. Bispectral analysis or bicoherence is a powerful tool in signal processing which offers a way to analyze the nonlinear coupling between frequencies and helps us in areas where linear power spectral analysis provides insufficient information [46]. Bicoherence analysis was used to investigate the nonlinearities in the aeroelastic systems [47]. The nonlinear aspects of the aerodynamic loading are determined from estimates of higher-order spectral moments, namely, the auto- and cross-bispectrum through which the quadratic nonlinear interaction between two frequency components are calculated and are used to detect a quadratic coupling or interaction among different frequency components of a signal [47].

Bicoherence is the squared normalized version of bispectral density. Bicoherence gives a measure of phase coupling between signals at three different frequencies. Bicoherence is mostly used in fault diagnosis because of its ability to trace and analyze multifrequency components. It is most effective in analyzing systems with nonlinear coupling between frequencies and is useful in detecting and quantifying the presence of nonlinearity, thus indicating the severity of the fault in the machine [48, 49]. Bicoherence is also considered as a tool to analyze the coupling effects between states of a dynamical system at different frequencies [50–52].

The power spectrum of a discrete time series $x(n)$ is given by

$$P_{xx}(k) = E[x(k)x_*(k)], \quad (6)$$

where k is the discrete frequency variable. The bispectrum can be defined by

$$B_x(k,l) = E[x(k)x(l)x_*(k+l)]. \quad (7)$$

The bicoherence is the normalized bispectrum given by

$$b^2(k,l) = \frac{[E[x(k)x(l)x_*(k+l)]]^2}{E[x(k)x(l)]^2 E[x(k+l)]^2}. \quad (8)$$

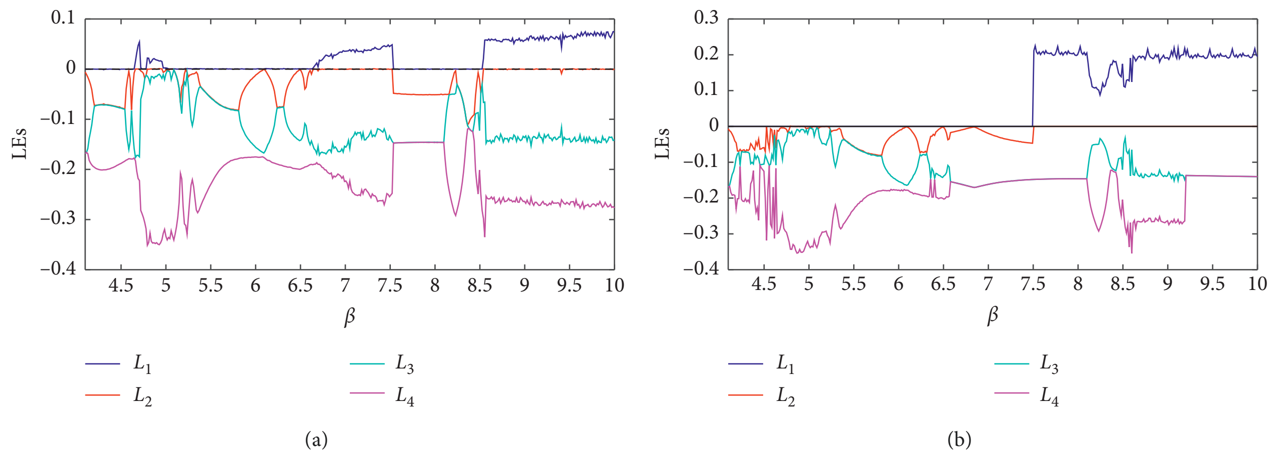

Figure 5: Lyapunov exponents for (a) forward continuation and (b) backward continuation.

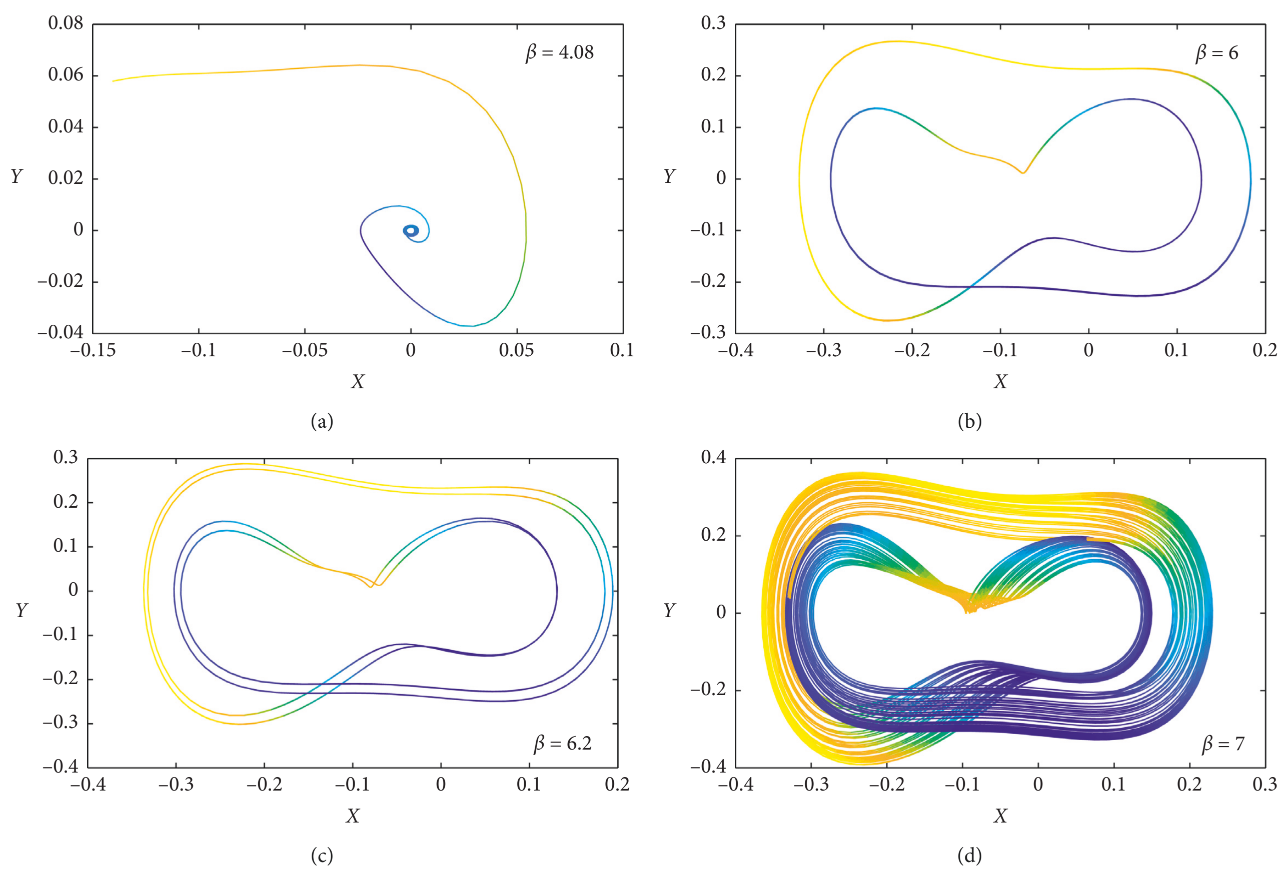

Figure 6: Phase portraits in the X-Y plane for various values of β: (a) point attractor; (b) period-1 limit cycle; (c) period-2 limit cycle; (d) chaotic attractor.

The cross bicoherence can be calculated by using the following definition:

$$b_{xy}{}^{2}(k,l) = \frac{\left[E\left[x(k)x(l)y_{*}(k+l)\right]\right]^{2}}{E\left[x(k)x(l)\right]^{2}E\left[y(k+l)\right]^{2}}. \tag{9}$$

The bicoherence at any frequency pair $k+l$ can be interpreted as the fraction of power at frequency $k+l$ which is phase coupled to the component at $k+l$. We have used the Welch periodogram method to estimate the bispectrum of the airfoil system (ASHS) and then the bicoherence, but the lengths of data required to obtain consistent estimates are longer than those required for power spectrum estimation; hence, we sampled the time series data generated from the ASHS state equations at 1 KHz and have used 30,000 samples for the bicoherence analysis.

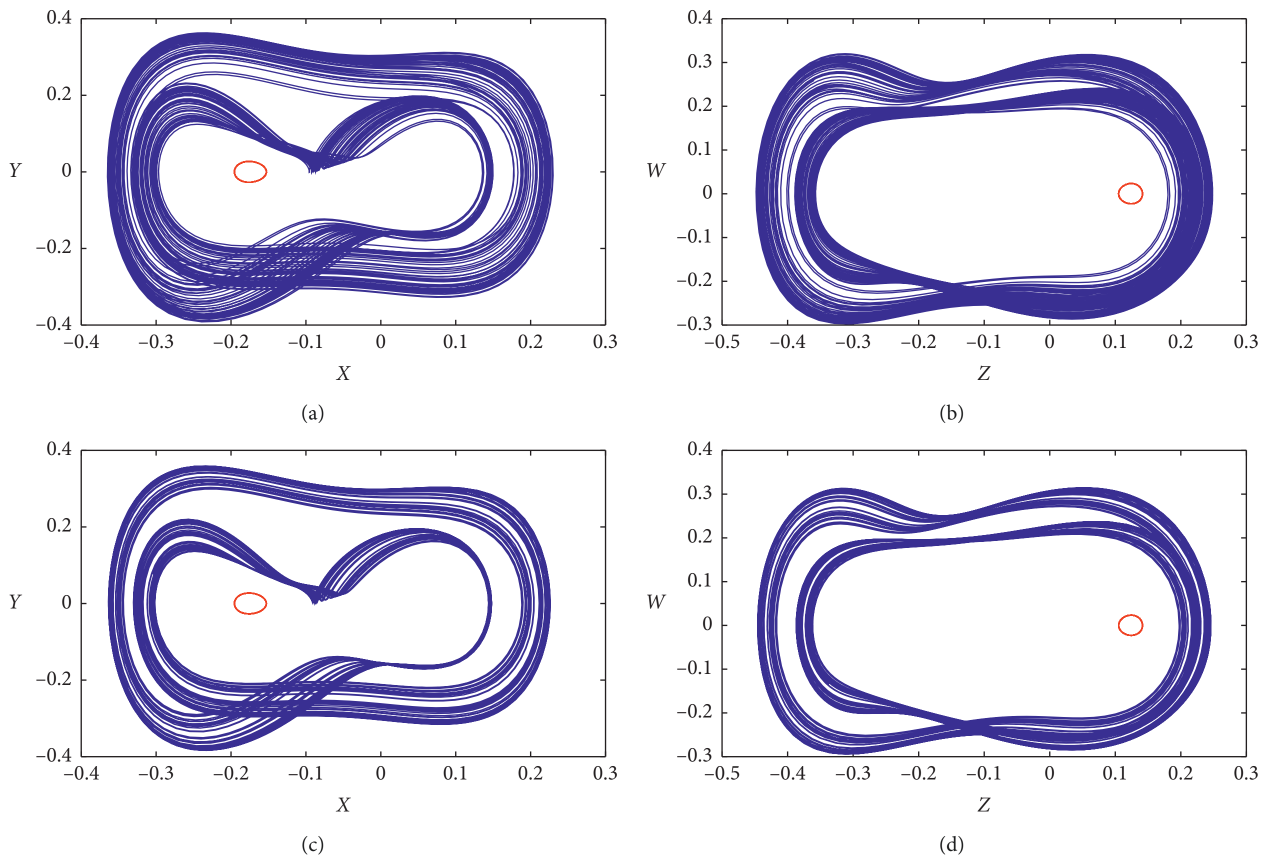

Figure 7: Coexisting attractors for different values of β: for $\beta = 5$ and initial conditions for (a, b) blue $[-0.012, -0.055, 0.009, -0.125]$; red $[-0.13, 0, 0.09, 0]$; for $\beta = 7$ and initial conditions for (c, d) blue $[-0.09, 0.003, 0.13, 0.22]$; red $[-0.17, 0.02, 0.13, -0.02]$.

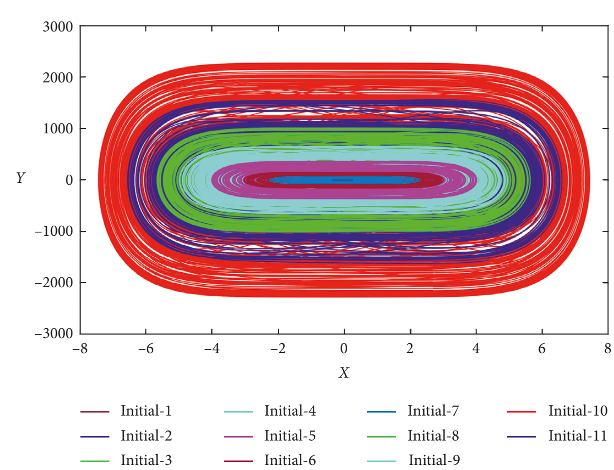

Figure 8: Multiple coexisting attractors for $\beta = 7$ with different initial conditions $[P, 0, 0.1, 0]$ where P takes the values of $[0.5, 1, 2, 3, 4, 5, 6, 7, 8, 9, 10]$ for initial-1 to initial-11, respectively.

We have presented the bicoherence plots of the ASHS for different values of the parameter β as shown in Figure 9. We could see that the coupling between states are much weaker for $\beta = 4.1$ but becomes stronger (yellow spots) for $\beta = 4.6$ and $\beta = 5$ and forms multiple islands of small bandwidths for $\beta = 7$ indicating the strength of the coupling effects of the frequencies. We have used a fixed initial condition of $[0.1, 0, 0.1, 0]$. The bicoherence spectrum of surface elevations at the first measured location (Figure 9) far from the focal location indicates that many wave modes were involved in the wave-wave interactions. The bicoherence ($\beta = 5$) at $b^2(0.16, 0.16) = 1.4$ denotes a self wave-wave interactions, while $b^2(0.16, 0.12) = 1.4$ denotes a nonlinear coupling between two different frequencies.

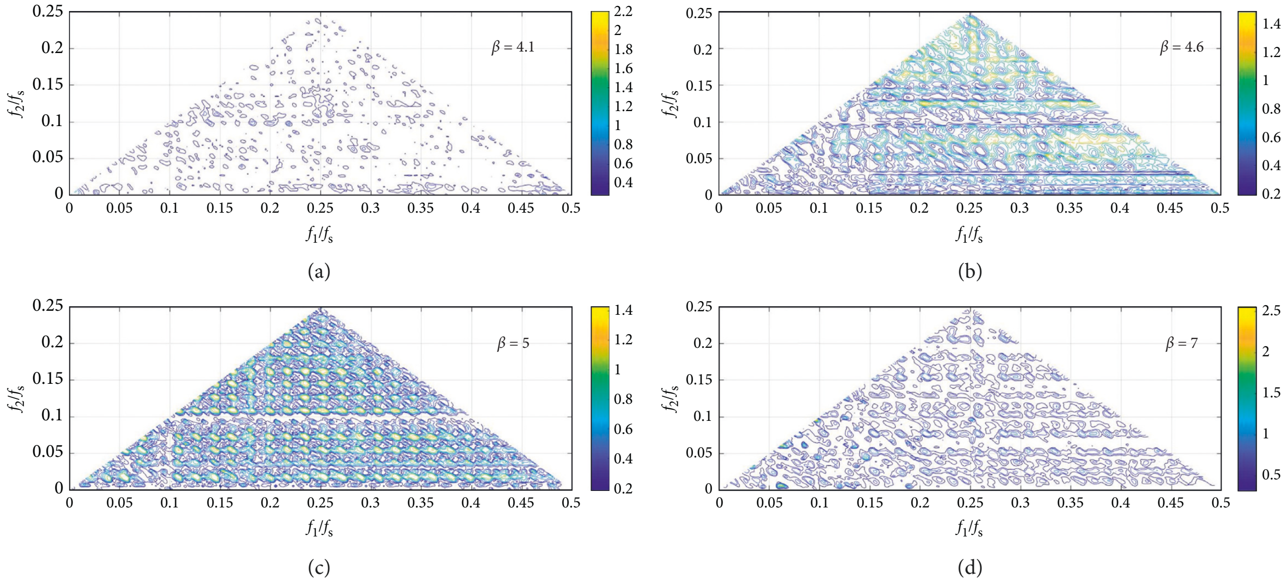

FIGURE 9: Bicoherence plots of the ASHS.

4. Conclusion

We have modified the dynamics of the well-known airfoil system by introducing higher-order nonlinearity in plunging and pitching stiffnesses. Chaotic motions exist in an airfoil system when the airspeed exceeds the critical divergent speed. The dynamical analysis of the proposed model shows unique characters of multistability and infinitely coexisting attractors known as megastability. Such features of an airfoil system were not captured earlier in the literatures. Bicoherence plots are investigated to know the impact of multifrequency terms and coupled nonlinearities on the system.

Data Availability

All the numerical simulation parameters are mentioned in the respective text part, and there are no additional data requirements for the simulation results.

Conflicts of Interest

The authors declare that they have no conflicts of interest.

References

[1] J. J. Block and T. W. Strganac, "Applied active control for a nonlinear aeroelastic structure," *Journal of Guidance, Control, and Dynamics*, vol. 21, no. 6, pp. 838–845, 1998.

[2] K. Palaniappan, P. Sahu, J. J. Alonso, and A. Jameson, "Design of adjoint based laws for wing flutter control," in *Proceedings of the 47th AIAA Aerospace Sciences Meeting and Exhibit*, Orlando, Florida, January 2009.

[3] V. V. Golubev, B. D. Dreyer, T. M. Hollenshade, and M. Visbal, "High-accuracy viscous simulations of gust-airfoil nonlinear aeroelastic interaction," in *Proceedings of the 39th AIAA Fluid Dynamics Conference*, San Antonio, TX, USA, June 2009.

[4] M. L. Tharayil and A. G. Alleyne, "Modeling and control for smart mesoflap aeroelastic controlflap aeroelastic control," *IEEE/ASME Transactions on Mechatronics*, vol. 9, no. 1, pp. 30–39, 2004.

[5] L. C. Zhao and Z. C. Yang, "Chaotic motions of an airfoil with non-linear stiffness in incompressible flow," *Journal of Sound and Vibration*, vol. 138, no. 2, pp. 245–254, 1990.

[6] J.-K. Liu and L.-C. Zhao, "Bifurcation analysis of airfoils in incompressible flow," *Journal of Sound and Vibration*, vol. 154, no. 1, pp. 117–124, 1992.

[7] T. O'Neill and T. W. Strganac, "Aero elastic response of a rigid wing supported by nonlinear spring," *Journal of Aircraft*, vol. 35, no. 4, pp. 616–622, 1998.

[8] Y. C. Fung, *An Introduction to the Theory of Aeroelasticity*, Wiley, New York, NY, USA, 1955.

[9] T. Theodorsen and I. E. Garrick, "Mechanism of flutter: a theoretical and experiment investigation of the flutter problem," Report No. 685, NACA, Boston, MA, USA, 1940.

[10] T. W. Strganac, J. Ko, and D. E. Thompson, "Identification and control of limit cycle oscillations in aeroelastic systems," *Journal of Guidance, Control, and Dynamics*, vol. 23, no. 6, pp. 1127–1133, 2000.

[11] B. H. K. Lee, S. J. Price, and Y. S. Wong, "Nonlinear aeroelastic analysis of airfoils: bifurcation and chaos," *Progress in Aerospace Sciences*, vol. 35, no. 3, pp. 205–334, 1999.

[12] D.-M. Zhao and Qi-C. Zhang, "Bifurcation and chaos analysis for aeroelastic airfoil with freeplay structural nonlinearity in pitch," *Chinese Physics B*, vol. 19, no. 3, Article ID 030518, 2010.

[13] Z. Yang, S. He, and Y. Gu, "Transonic limit cycle oscillation behavior of an aeroelastic airfoil with free-play," *Journal of Fluids and Structures*, vol. 66, pp. 1–18, 2016.

[14] S. He, Z. Yang, and Y. Gu, "Nonlinear dynamics of an aeroelastic airfoil with free-play in transonic flow," *Nonlinear Dynamics*, vol. 87, no. 4, pp. 2099–2125, 2017.

[15] D. A. Pereira, R. M. G. Vasconcellos, M. R. Hajj, and F. D. Marques, "Effects of combined hardening and free-play nonlinearities on the response of a typical aeroelastic section," *Aerospace Science and Technology*, vol. 50, pp. 44–54, 2016.

[16] H. Dai, X. Yue, J. Yuan, D. Xie, and S. N. Atluri, "A comparison of classical Runge-Kutta and Henon's methods for capturing chaos and chaotic transients in an aeroelastic system with freeplay nonlinearity," *Nonlinear Dynamics*, vol. 81, no. 1-2, pp. 169–188, 2015.
[17] H.-l. Guo and Y.-s. Chen, "Dynamic analysis of two-degree-of-freedom airfoil with freeplay and cubic nonlinearities in supersonic flow," *Applied Mathematics and Mechanics*, vol. 33, no. 1, pp. 1–14, 2012.
[18] J. T. Gordon, E. E. Meyer, and R. L. Minogue, "Nonlinear stability analysis of control surface flutter with freeplay effects," *Journal of Aircraft*, vol. 45, no. 6, pp. 1904–1916, 2008.
[19] D. Zhao, Q. Zhang, and Y. Tan, "Random flutter of a 2-DOF nonlinear airfoil in pitch and plunge with freeplay in pitch," *Nonlinear Dynamics*, vol. 58, no. 4, pp. 643–654, 2009.
[20] C. C. Cui, J. K. Liu, and Y. M. Chen, "Simulating nonlinear aeroelastic responses of an airfoil with freeplay based on precise integration method," *Communications in Nonlinear Science and Numerical Simulation*, vol. 22, no. 1–3, pp. 933–942, 2015.
[21] W. J. Al-Mashhadani, E. H. Dowell, H. R. Wasmi, and A. A. Al-Asadi, "Aeroelastic response and limit cycle oscillations for wing-flap-tab section with freeplay in tab," *Journal of Fluids and Structures*, vol. 68, pp. 403–422, 2017.
[22] E. Verstraelen, G. Dimitriadis, G. D. B. Rossetto, and E. H. Dowell, "Two-domain and three-domain limit cycles in a typical aeroelastic system with freeplay in pitch," *Journal of Fluids and Structures*, vol. 69, pp. 89–107, 2017.
[23] N. Ebrahimzade, M. Dardel, and R. Shafaghat, "Performance comparison of linear and nonlinear vibration absorbers in aeroelastic characteristics of a wing model," *Nonlinear Dynamics*, vol. 86, no. 2, pp. 1075–1094, 2016.
[24] Y. Bichiou, M. R. Hajj, and A. H. Nayfeh, "Effectiveness of a nonlinear energy sink in the control of an aeroelastic system," *Nonlinear Dynamics*, vol. 86, no. 4, pp. 2161–2177, 2016.
[25] F. Chen, L. Zhou, and Y. Chen, "Bifurcation and chaos of an airfoil with cubic nonlinearity in incompressible flow," *Science China Technological Sciences*, vol. 54, no. 8, pp. 1954–1965, 2011.
[26] M. Cai, J.-k. Liu, and J. Li, "Incremental harmonic balance method for airfoil flutter with multiple strong nonlinearities," *Applied Mathematics and Mechanics*, vol. 27, no. 7, pp. 953–958, 2006.
[27] D. Poirel and S. J. Price, "Bifurcation characteristics of a two-dimensional structurally non-linear airfoil in turbulent flow," *Nonlinear Dynamics*, vol. 48, no. 4, pp. 423–435, 2007.
[28] A. Behal, P. Marzocca, V. M. Rao et al., "Nonlinear adaptive control of an aeroelastic two-dimensional lifting surface," *Journal of Guidance, Control, and Dynamics*, vol. 29, no. 2, pp. 382–390, 2006.
[29] C.-C. Wang, C.-L. Chen, and H.-T. Yau, "Terminal sliding mode control for aeroelastic systems," *Nonlinear Dynamics*, vol. 70, no. 3, pp. 2015–2026, 2012.
[30] C.-C. Wang, C.-L. Chen, and H.-T. Yau, "Bifurcation and chaotic analysis of aeroelastic systems," *Journal of Computational and Nonlinear Dynamics*, vol. 9, no. 2, Article ID 021004, 2013.
[31] X.-z. Xu, W.-x. Wu, and W.-g. Zhang, "Sliding mode control for a nonlinear aeroelastic system through backstepping," *Journal of Aerospace Engineering*, vol. 31, no. 1, Article ID 04017080, 2018.
[32] H. Guo, S. Cao, T. Yang, and Y. Chen, "Aeroelastic suppression of an airfoil with control surface using nonlinear energy sink," *Nonlinear Dynamics*, vol. 94, no. 2, pp. 857–872, 2018.
[33] P. S. Beran, C. L. Pettit, and D. R. Millman, "Uncertainty quantification of limit-cycle oscillations," *Journal of Computational Physics*, vol. 217, no. 1, pp. 217–247, 2006.
[34] J. C. Sprott, "A proposed standard for the publication of new chaotic systems," *International Journal of Bifurcation and Chaos*, vol. 21, no. 9, pp. 2391–2394, 2011.
[35] Y. C. Kim and E. J. Powers, "Digital bispectral analysis and its applications to nonlinear wave interactions," *IEEE Transactions on Plasma Science*, vol. 7, no. 2, pp. 120–131, 1979.
[36] K. Rajagopal, A. Karthikeyan, P. Duraisamy, and R. Weldegiorgis, "Bifurcation and chaos in integer and fractional order two-degree-of-freedom shape memory alloy oscillators," *Complexity*, vol. 2018, Article ID 8365845, 9 pages, 2018.
[37] K. Rajagopal, D. Prakash, R. Weldegiorgis, and A. Karthikeyan, "Multistability in horizontal platform system with and without time delays," *Shock and Vibration*, vol. 2018, Article ID 1092812, 8 pages, 2018.
[38] A. Wolf, J. B. Swift, H. L. Swinney, and J. A. Vastano, "Determining Lyapunov exponents from a time series," *Physica D: Nonlinear Phenomena*, vol. 16, no. 3, pp. 285–317, 1985.
[39] S. P. Dawson, C. Grebogi, J. A. Yorke, I. Kan, and H. Koçak, "Antimonotonicity: inevitable reversals of period-doubling cascades," *Physics Letters A*, vol. 162, no. 3, pp. 249–254, 1992.
[40] J. C. Sprott, S. Jafari, A. J. M. Khalaf, and T. Kapitaniak, "Megastability: coexistence of a countable infinity of nested attractors in a periodically-forced oscillator with spatially-periodic damping," *The European Physical Journal Special Topics*, vol. 226, no. 9, pp. 1979–1985, 2017.
[41] Z. Wang, H. R. Abdolmohammadi, F. E. Alsaadi, T. Hayat, and V.-T. Pham, "A new oscillator with infinite coexisting asymmetric attractors," *Chaos, Solitons & Fractals*, vol. 110, pp. 252–258, 2018.
[42] Y.-X. Tang, A. J. M. Khalaf, K. Rajagopal, V.-T. Pham, S. Jafari, and Y. Tian, "A new nonlinear oscillator with infinite number of coexisting hidden and self-excited attractors," *Chinese Physics B*, vol. 27, no. 4, Article ID 040502, 2018.
[43] Y. Tang, H. R. Abdolmohammadi, A. J. M. Khalaf, Y. Tian, and T. Kapitaniak, "Carpet oscillator: a new megastable nonlinear oscillator with infinite islands of self-excited and hidden attractors," *Pramana*, vol. 91, no. 1, p. 11, 2018.
[44] H. Jahanshahi, K. Rajagopal, A. Akgul, N. N. Sari, H. Namazi, and S. Jafari, "Complete analysis and engineering applications of a megastable nonlinear oscillator," *International Journal of Non-Linear Mechanics*, vol. 107, pp. 126–136, 2018.
[45] P. Prakash, K. Rajagopal, J. P. Singh, and B. K. Roy, "Megastability in a quasi-periodically forced system exhibiting multistability quasi-periodic behavior, and its analogue circuit simulation," *AEU-International Journal of Electronics and Communications*, vol. 92, pp. 111–115, 2018.
[46] J. W. A. Fackrell, P. R. White, J. K. Hammond, R. J. Pinnington, and A. T. Parsons, "The interpretation of the bispectra of vibration signals—: I. Theory," *Mechanical Systems and Signal Processing*, vol. 9, no. 3, pp. 257–266, 1995.
[47] W. Silva, "Identification of nonlinear aeroelastic systems based on the volterra theory: progress and opportunities," *Nonlinear Dynamics*, vol. 39, no. 1-2, pp. 25–62, 2005.
[48] E. B. Halim, S. L. Shah, M. A. A. S. Choudhury, and R. Kadali, "Application of bicoherence analysis on vibration data for condition based monitoring of rotating machinery," *IFAC Proceedings Volumes*, vol. 41, no. 2, pp. 4517–4522, 2018.

[49] E. B. Halim, M. A. A. S. Choudhury, S. L. Shah, and M. J. Zuo, "Fault detection of rotating machinery from bicoherence analysis of vibration data," *IFAC Proceedings Volumes*, vol. 39, no. 13, pp. 1348–1353, 2006.

[50] K. Rajagopal, G. Laarem, A. Karthikeyan, A. Srinivasan, and G. Adam, "Fractional order memristor no equilibrium chaotic system with its adaptive sliding mode synchronization and genetically optimized fractional order PID synchronization," *Complexity*, vol. 2017, Article ID 1892618, 19 pages, 2017.

[51] K. Rajagopal, A. Karthikeyan, and A. K. Srinivasan, "FPGA implementation of novel fractional order chaotic systems with two equilibriums and no equilibrium and its adaptive sliding mode synchronization," *Nonlinear Dynamics and Chaos in Engineering systems*, Springer, vol. 87, no. 4, pp. 2281–2304, 2017.

[52] K. Rajagopal, L. Guessas, S. Vaidyanathan, A. Karthikeyan, and A. Srinivasan, "Dynamical analysis and FPGA implementation of a novel hyperchaotic system and its synchronization using adaptive sliding mode control and genetically optimized PID control," *Mathematical Problems in Engineering*, vol. 2017, no. 1, Article ID 7307452, 14 pages, 2017.